# A new method for determining the meridional wind velocity during an ionospheric storm

Zhigang Yuan, Baiqi Ning, Libo Liu, Weixing Wan, and Biqiang Zhao

Wuhan Ionospheric Observatory, Wuhan Institute of Physics and Mathematics, Chinese Academy of Sciences, Wuhan, China

Received 17 October 2002; revised 20 January 2003; accepted 7 February 2003; published 21 March 2003.

[1] This paper introduces a new method for determining the meridional wind velocity during an ionospheric storm based on a sequence of Doppler ionograms. By this new method, the height- and time-dependent meridional wind velocity in the $F_2$ layer was obtained during the magnetic substorm on April 17, 2002. The peak velocity of meridional wind at 300 km altitude is about 300 m/s, the deduced propagation velocity of traveling atmospheric disturbances (TADs) is about 520 m/s. Furthermore, not only the amplitude but also the onset time and phase velocity of the TAD-associated wind perturbation can be explained by the present theories and observations of meridional winds. This work offers a new method to investigate the propagation and morphology of meridional wind during a magnetic substorm by using Digisonde routine observations. *INDEX TERMS:* 2435 Ionosphere: Ionospheric disturbances; 2437 Ionosphere: Ionospheric dynamics; 2487 Ionosphere: Wave propagation (6934); 2494 Ionosphere: Instruments and techniques. **Citation:** Yuan, Z., B. Ning, L. Liu, W. Wan, and B. Zhao, A new method for determining the meridional wind velocity during an ionospheric storm, *Geophys. Res. Lett.*, *30*(6), 1290, doi:10.1029/2002GL016469, 2003.

## 1. Introduction

[2] It is well known that during a substorm-associated energy injection at polar latitudes, gravity waves are generated. At some distance from the source region these waves will superimpose to form an impulse-like perturbation, which moves with high velocity from polar to equatorial latitudes [e.g., *Testud et al.*, 1975; *Prölss and Jung*, 1978; *Roble et al.*, 1978; *Crowley et al.*, 1989; *Bauske and Prölss*, 1997]. Traveling atmospheric disturbances (TADs) that carry along equatorward-directed meridional winds of moderate magnitude propagate from polar to equatorial latitudes, possibly causing ionospheric storms at middle or low latitudes during a magnetic substorm [e.g., *Fesen et al.*, 1989; *Burns and Killeen*, 1992; *Fuller-Rowell et al.*, 1994; *Lee et al.*, 2002; *Prölss*, 1982].

[3] In this work, we are interested in TADs that propagate equatorward in the East Asian region during a magnetic substorm. In order to investigate TAD effects, data obtained by a Digisonde 256 [*Reinisch*, 1996] at Wuhan (30.6°N, 114.4°E, magnetic dip: 45.2°) were analyzed for the April 17, 2002 disturbance event. The measurements of the F layer critical frequency $foF_2$ (or plasma density $NmF_2$) and the F-peak height $hmF_2$ are used to document the ionospheric response to the substorm. As a measure of the degree of perturbation during the storm, we define $\delta f_oF_2\%$, which represents the percent ratio of the difference between the geomagnetically disturbed day and the quiet days of the month to the $f_oF_2$ of the quiet day [*Danilov*, 2001]. From rapid sequence ionograms with highly accurate Doppler information, the meridional wind velocity during the ionospheric storm has been derived. At the same time, the meridional and vertical phase velocities of TADs are deduced by the Multiple-channel Maximum Entropy Method (MMEM). Furthermore, other parameters, including the magnitude of the meridional wind during this ionospheric storm, are examined and discussed.


0094-8276/03/2002GL016469$05.00

## 2. Determination of Meridional Wind Velocities

[4] For a large scale TAD, the meridional components of the TAD's gradients are negligible in contrast to the vertical components due to the large horizontal wave length. The continuity equation can be simplified by assuming that the ionosphere is horizontally stratified and the net effect of chemical processes in the $F_2$ layer is negligible compared to the transport term during a large TAD [*Bertel et al.*, 1984]. It then reduces to

$$\frac{\partial N_e}{\partial t} = -\left(N_e \frac{\partial V_{ez}}{\partial z} + \frac{\partial N_e}{\partial z} V_{ez}\right) \tag{1}$$

where $V_{ez}$ represents the vertical component of the electron drift velocity, and $N_e$ is the electron density. *Wan and Li* [1993] showed that the normal velocity vector, $\boldsymbol{V}$, of iso-electron density surfaces is defined as the ratio between the rates of temporal and spatial variation of $N_e$, and the vertical component of $\boldsymbol{V}$ becomes

$$V_z = -\frac{\partial N_e / \partial t}{\partial N_e / \partial z} \qquad \frac{\partial N_e}{\partial z} \neq 0 \tag{2}$$

Combining (1) and (2) gives

$$V_z = \left(\frac{N_e}{\partial N_e / \partial z}\right)\left(\frac{\partial V_{ez}}{\partial z}\right) + V_{ez} \tag{3}$$

[5] When a TAD passes, its winds drag the ionization along the inclined magnetic field lines. In this paper, we only pay attention to the winds at $F_2$ region heights. The relationship between the neutral wind velocity $\boldsymbol{V_n}$ and the

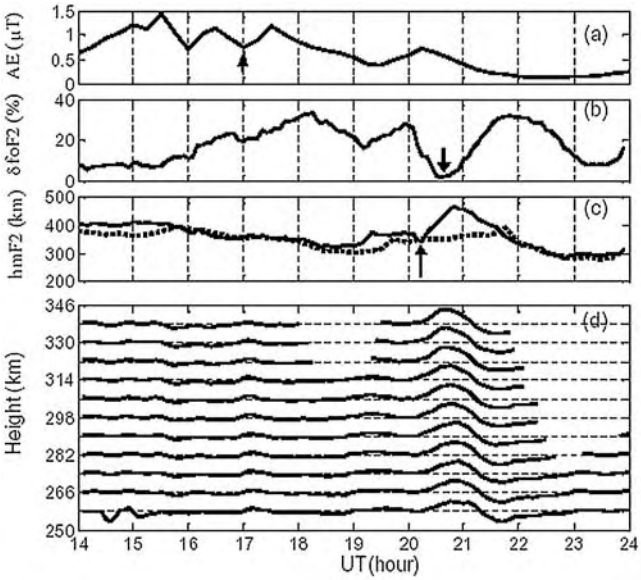


**Figure 1.** Variation of the ionospheric parameters, the inferred meridional winds, and the AE index with time. (a) AE index. (b) (c)$\delta f_oF_2$% and $hmF_2$ respectively observed at Wuhan on April 17, 2002 (solid lines), the quiet-time $hmF_2$ is a reference (dotted lines). (d) the inferred meridional winds from Doppler ionograms. A height interval of 8 km corresponds to a velocity interval of 400 m/s.

ion drift velocity $\boldsymbol{V_i}$ reduces approximately to [*Hooke*, 1970]

$$\boldsymbol{V_i} \approx (\boldsymbol{V_n} \cdot \mathbf{I_b})\mathbf{I_b} \tag{4}$$

where $\mathbf{l}_b$ is a unit vector directed parallel to the geomagnetic field. Using equation (4) and ignoring the vertical component of the neutral wind and under the condition of charge neutrality ($V_i = V_e$), equation (3) can be written as

$$V_z = \sin \mathrm{I} \cos \mathrm{I} \left[ \left( \frac{N_e}{\partial N_e / \partial z} \right) \left( \frac{\partial V_m}{\partial z} \right) + V_m \right] \tag{5}$$

where I is the geomagnetic inclination, and $V_m$ denotes the horizontal meridional wind velocity. By inversing equation (5) it is possible to derive the meridional wind velocity during a substorm.

[6] Usually, Doppler ionograms can be used to infer the vertical motion of plasma contours under some circumstance [*Wright and Pitteway*, 1982, 1994; *Parkinson et al.*, 1999]. Our recent work uses the highly accurate Doppler ionograms recorded during routine operation of the Digisonde 256 [Yuan et al., Acquirement and analysis of highly accurate Doppler ionogram from Digisonde observation, submitted to *Radio Sci.*, 2002]. From these Doppler ionograms, $V_z$ for each sounding frequency is derived by a multiple frequency Doppler inversion technique [*Wan and Li*, 1993]. Then using the profiles of the ionospheric electron density [*Reinisch and Huang*, 1983], $V_z$ at different heights can be obtained by an interpolation technique. After a sequence of Doppler ionograms is processed, $V_z$ is deduced as a function of height and time (Yuan et al., submitted manuscript, 2002). In terms of equation (5), by using a piecewise linear function of the sounding frequency f to approximate the function $V_m(f)$, the height- and time-dependant meridional wind velocity $V_m$ can be derived [*Wan and Li*, 1993], which are shown in Figure 1. Because the Doppler shifts can only be measured for the sounding frequencies lower than $f_oF_2$, the data is missing at some heights in Figure 1 due to lower $hmF_2$.

## 3. Analysis and Discussion

[7] In order to study the ionospheric storm, we first consider the AE index. According to Figure 1, the AE index begins to rise at 1400 UT (2200 LT) and remains above the 0.5μT level for four consecutive hours. The associated ionospheric effect at Wuhan is of comparable duration, as the arrows show in Figure 1, its onset (a lifting of $hmF_2$) lags the rise in substorm activity by about 3 hours. Considering that the source in the auroral oval (75°N) is about 4940 km away from Wuhan (30.6°N) at the same longitude [*Prölss*, 1993], this corresponds to an average disturbance propagation velocity of about 460 m/s. Furthermore the increase in ionization density lags the uplifting of the $F_2$ layer, by about forty minutes. We note that the inferred meridional wind during the ionospheric storm shows a good correlation with the AE index. Corresponding to high level of AE index during 1400–1800 UT, the inferred meridional wind velocity shows three surge-like disturbances during 1700–2100 UT. Here we focus on the disturbance during 2000–2100 UT because it is more distinct than the others. This surge-like disturbance has two major characteristics. Firstly, it is obvious that there is a wavefront tilt of the disturbance, in agreement with previous observations [e.g., *Rüster*, 1965] and model calculations [e.g., *Richmond and Matsushita*, 1975; *Millward et al.*, 1993]. Secondly, as show in Figure 2 the height gradient of the disturbance amplitude is positive and tends to decrease with increasing altitude. The peak velocity at 300 km altitude is 300 m/s. Evidently the derived wind

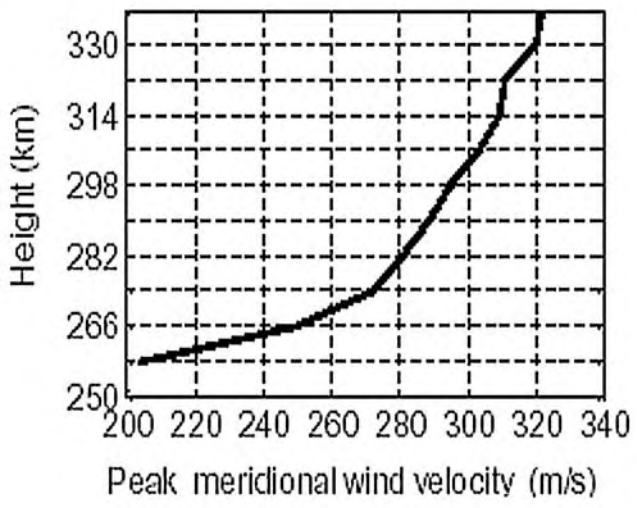


**Figure 2.** Variation of the derived peak meridional wind with height.

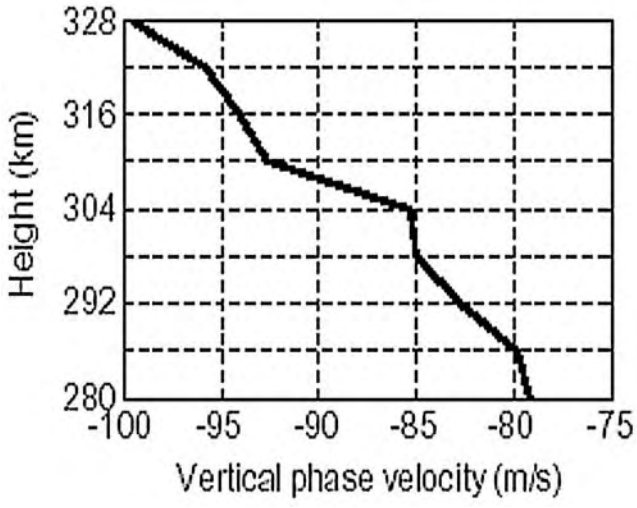


**Figure 3.** Variation of vertical phase velocity of the inferred meridional wind with height.

velocities are within a reasonable range and consistent with those derived by *Bauske and Prölss* [1997].

[8] Next, we deduce some parameters of the TAD observed during 2000–2100 UT on April 17. In order to get the spectra and phase with high precision and resolution from a short sequence of data, the MMEM has been used to extract disturbance parameters from the adjacent height data of TADs (Yuan et al., submitted manuscript, 2002). The calculated mean wave period of the TAD is 84 min. Figure 3 shows a downward direction of the phase velocity, which implies that the iso-phase surface is propagating from higher layers to lower layers. The vertical phase speed $|V_{pv}|$ tends to increase as height increases. We also deduce the mean $V_{pv}$ as −88 m/s. These preliminary results are in agreement with the theory of TADs [*Yeh and Liu*, 1974].

[9] Below the F-layer peak, most observations reveal that very large disturbances are simply free internal gravity waves with properties determined by the atmospheric parameters of the thermosphere [*Georges*, 1968]. The relationship can be expressed as

$$\cos\theta = {T_B}/{T} = {V_{pv}}/{\sqrt{V_{ph}^2 + V_{pv}^2}} \qquad (6)$$

where $T_B$ is the Brunt-Väisälä period which is about 14 min. in the thermosphere. θ is the angle of the wavefront with the vertical, and T is the wave period of the TAD. $V_{pv}$ and $V_{ph}$ are the vertical and horizontal components of the phase velocity, respectively. From equation (6), we determine $V_{ph}$ to be about 520 m/s, a value consistent with the propagation velocity (about 600 m/s) suggested by *Prölss* [1993]. As we know, this $V_{ph}$ could be considered as the propagation velocity of a TAD from high to low latitudes during the substorm, which occurred at about 1730 UT on April 17. On the other hand, $V_{ph}$ can be roughly derived from the time lag between the peak of the AE index at about 1730 UT and the peak of the meridional wind velocity at about 2030 UT. The derived $V_{ph}$ is about 460 m/s, which is consistent with the result in terms of equation (6). The result implies that a magnetospheric substorm causes a surge-like TAD, which propagates with a high velocity of about 500 m/s from polar to equatorial latitudes, and that meridional wind produces a positive ionospheric storm effect, indicated here by the anomalous increase of $NmF_2$ at about 2100 UT.

## 4. Summary

[10] In this paper, we introduced a new method for determining the meridional wind velocity during an ionospheric storm using a sequence of Doppler ionograms. A height- and time-dependent meridional wind in the $F_2$ layer was obtained during the magnetic substorm on April 17, 2002. The result shows that the inferred parameters of the TAD, including the disturbance amplitude and propagating velocity, are reasonable. Also the amplitude, onset time, and propagation velocity of the TAD-associated wind perturbation can be explained by the present theory and observations of meridional winds. It should be kept in mind that this new method is limited by some factors: (1) the Doppler shifts can not be acquired for the sounding frequencies above $f_oF_2$; (2) the aligned component of the diffusion term also has an influence on the determination of the meridional wind velocity [*Millward et al.*, 1993]; (3) the photochemical effects play an important role in lower ionosphere [*Hooke*, 1968; *Davies*, 1990]. All in all, this work offers a new method to determine the meridional wind during ionospheric storms. With this method it becomes possible to further study the propagation and morphology of meridional winds during a magnetic substorm by routine Digisonde observations.. Furthermore, we can obtain the meridional wind above the $F_2$ layer peak if the derived wind is connected with a wind model [e.g., *Richmond and Matsushita*, 1975; *Millward et al.*, 1993], a method that will be discussed in a later paper.

[11] **Acknowledgments.** This research is supported by National Key Research Project (G2000078407) and Natural Science Foundation of China (40134020, 40274054). The authors would like to thank the referees for valuable suggestions that greatly improved the presentation of the paper.

## References

Bauske, R., and W. G. Prölss, Modeling the ionospheric response to traveling atmospheric disturbances, *J. Geophys. Res.*, *102*, 14,555–14,562, 1997.

Bertel, L., P. Guyader, and P. Lassudrie-Duchesne, Multiple-frequency Doppler sounding of the ionosphere: Theory and experimental comparison with incoherent scatter results, *Radio Sci.*, *19*, 879–890, 1984.

Burns, J. D., and T. L. Killeen, The equatorial neutral thermospheric response to geomagnetic forcing, *Geophys. Res. Lett.*, *19*, 977–980, 1992.

Crowley, G., B. A. Emery, R. G. Roble, H. C. Carlson Jr., and D. J. Knipp, Thermospheric dynamics during September 18–19, 1984, I, Model simulations, *J. Geophys. Res.*, *94*, 16,925–16,944, 1989.

Danilov, A. D., F2-region response to geomagnetic disturbances, *J. Atmos. Solar Terr. Phys.*, *63*, 441–449, 2001.

Davies, K., Ionospheric Radio, IEE Electromagnetic Waves Series 31, Peter Peregrinus Ltd., London, United Kingdom, 1990.

Fesen, C. G., G. Crowley, and R. G. Roble, Ionospheric effects at low latitudes during the March 22, 1979, geomagnetic storm, *J. Geophys. Res.*, *94*, 5405–5417, 1989.

Fuller-Rowell, T. J., M. V. Codrescu, R. J. Moffett, and S. Quegan, Response of the thermospheric and ionospheric to geomagnetic storms, *J. Geophys. Res.*, *99*, 3893–3914, 1994.

Georges, T. M., HF Doppler studies of traveling ionospheric disturbances, *J. Atmos. Terr. Phys.*, *30*, 735–746, 1968.

Hooke, W. H., Ionospheric irregularities produced by internal atmospheric gravity waves, *J. Atmos. Terr. Phys.*, *30*, 795–823, 1968.

Hooke, W. H., The ionospheric response to internal gravity waves 1. the F2 region response, *J. Geophys. Res.*, *75*, 5535–5544, 1970.

Lee, C. C., J. Y. Liu, B. W. Reinisch, Y. P. Lee, and L. B. Liu, The propagation of traveling atmospheric disturbances observed during the

April 6–7, 2000 ionospheric storm, *Geophys. Res. Lett.*, *29*(5), doi:10.1029/2001GL013516, 2002.

Millward, G. H., R. J. Moffett, S. Quegan, and T. J. Fuller-Rowell, Effects of an atmospheric gravity waves on the midlatitude ionospheric F layer, *J. Geophys. Res.*, *98*, 19,173–19,179, 1993.

Parkinson, M. L., A. M. Breed, P. L. Dyson, and R. J. Morris, Application of the Doppler ionogram to Doppler-sorted interferometry measurements of ionospheric drift velocity, *Radio Sci*, *34*(4), 899–912, 1999.

Prölss, G. M., Perturbation of the low-latitude upper atmosphere during magnetic substorm activity, *J. Geophys. Res.*, *87*, 5260–5266, 1982.

Prölss, G. W., On explaining the local time variation of ionospheric storm effects, *Ann. Geophys.*, *11*, 1–9, 1993.

Prölss, G. W., and M. J. Jung, Traveling atmospheric disturbances as a possible explanation for daytime positive storms effects of moderate duration at middle latitudes, *J. Atmos. Terr. Phys.*, *40*, 1351–1354, 1978.

Reinisch, B. W., Ionosonde, in *Upper Atmosphere, Data Analysis and Interpretation*, edited by W. Dieminger, G. K. Hartmann, and R. Leitinger, springer, 370–381, 1996.

Reinisch, B. W., and X. Huang, Automatic calculation of electron density profiles from digital ionograms, 3, Processing of bottomside ionograms, *Radio Sci*, *18*, 477–492, 1983.

Richmond, A. D., and S. Matsushita, Thermospheric response to a magnetic substorm, *J. Geophys. Res.*, *80*, 2839–2850, 1975.

Roble, R. G., A. D. Richmond, W. L. Oliver, and R. M. Harper, Ionospheric effects of the gravity wave launched by the September 18, 1974, sudden commencement, *J. Geophys. Res.*, *38*, 999–1009, 1978.

Rüster, R., Height variations of the F2-layer above Tsumeb during geomagnetic bay-disturbances, *J. Atmos. Terr. Phys.*, *27*, 1229–1245, 1965.

Testud, J., P. Amayenc, and M. Blanc, Middle and low-latitude effects of auroral disturbances from incoherent-scatter, *J. Atmos. Terr. Phys.*, *37*, 989–1009, 1975.

Wan, W., and J. Li, Spectral behavior of TIDs detected from rapids sequence ionograms, *J. Atmos. Terr. Phys.*, *55*, 47–55, 1993.

Wright, J. W., and M. L. V. Pitteway, Application of Dopplionograms and Gonionograms to atmospheric gravity waves disturbances in the ionosphere, *J. Geophys. Res.*, *87*, 1719–1721, 1982.

Wright, J. W., and M. L. V. Pitteway, High-resolution velocity determinations from the dynasonde, *J. Atmos. Terr. Phys.*, *56*(8), 961–977, 1994.

Yeh, K. C., and C. H. Liu, Acoustic-gravity waves in the upper atmosphere, *Reviews of Geophysics and Space Physics*, *12*, 193–215, 1974.

Z. Yuan, B. Ning, L. Liu, W. Wan, and B. Zhao, Wuhan Ionospheric Observatory, Wuhan Institute of Physics and Mathematics, Chinese Academy of Sciences, Wuhan 430071, China.